Chapter 1

ATLAS-EXOT-2016-27: an ATLAS monojet analysis (36.2 fb^{-1})

D. Sengupta

Abstract

We present the MADANALYSIS 5 implementation of the recent ATLAS-EXOT-2016-27 monojet search. This search allows us to probe various new physics scenarios featuring a dark matter particle through the so-called monojet channel in which the final-state signature consists in one highly-energetic jet recoiling against missing transverse energy carried by dark matter particles. The results are based on the analysis of a dataset of 36.2 fb^{-1} of proton-proton collisions recorded by the ATLAS detector with a center-of-mass energy of 13 TeV. The validation of our reimplementation relies on a comparison of our predictions with the official ATLAS results in the context of a supersymmetry-inspired simplified model in which the Standard Model is extended by a neutralino and a stop decaying into a charm quark and a neutralino.

1 Introduction

In this contribution, we present the validation of the implementation, in the MADANALYSIS 5 [1–3] framework, of the ATLAS-EXOT-2016-27 search for dark matter in the monojet channel [4]. This search is in particular sensitive to certain supersymmetric scenarios, dark matter setups and extra dimensional models. Each of those models can indeed predict, in specific realizations, the production of a pair of invisible particles in association with a highly-energetic jet (*i.e.*, the signature under consideration).

For our validation procedure, we focus on a compressed supersymmetric configuration in which the searched for signature arises from the associated production of a hard jet with a pair of invisible squarks that each decays into a soft light jet and a neutralino. This process is illustrated by the representative Feynman diagram of Fig. 1.1. The considered analysis is in particular sensitive to the case of a compressed light stop that decays into a charm quark and a neutralino (through a flavor-violating loop-induced subprocess),

$$pp \rightarrow j \, \tilde{t}^*\tilde{t} \rightarrow j \, c\tilde{\chi}_1^0 \bar{c}\tilde{\chi}_1^0 \,. \tag{1.1}$$

This decay mode of the top quark becomes especially relevant when the more standard decay channels involving either a top quark or a chargino are closed.

2 Description of the analysis

The ATLAS monojet analysis targets a final-state containing at least one very energetic jet that is assumed to originate from initial state radiation, as well as a certain amount of missing transverse energy E_T^{miss}. The analysis strategy is twofold, depending on the selection cut on the missing transverse energy. In a first series of ten signal regions (IM1, IM2, . . ., IM10), it considers inclusive missing transverse energy selections,

$$E_T^{\mathrm{miss}} > E_{\mathrm{threshold}} \,, \tag{1.2}$$

where the 10 different thresholds range from 250 GeV to 1 TeV, as shown on the first line of the table of Fig. 1.2. In a second series of signal regions, the analysis instead considers exclusive missing tranverse energy selection,

$$E_{\mathrm{threshold}}^{\mathrm{min}} \leq E_T^{\mathrm{miss}} \leq E_{\mathrm{threshold}}^{\mathrm{max}} \,. \tag{1.3}$$
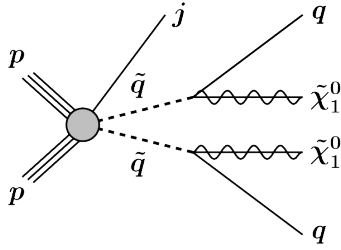
Fig. 1.1: Representative Feynman diagram corresponding to the production of a pair of squarks $\tilde{q}$ that each decays into a neutralino $\tilde{\chi}_1^0$ and a light quark q.

Inclusive (IM)	IM1	IM2	IM3	IM4	IM5	IM6	IM7	IM8	IM9	IM10
E_T^{miss} [GeV]	>250	>300	>350	>400	>500	>600	>700	>800	>900	>1000
Exclusive (EM)	EM1	EM2	EM3	EM4	EM5	EM6	EM7	EM8	EM9	EM10
E_T^{miss} [GeV]	250–300	300–350	350–400	400–500	500–600	600–700	700–800	800–900	900–1000	>1000

Fig. 1.2: Missing transverse energy requirements of the 20 signal regions of the ATLAS-EXOT-2016-27 analysis.

The thresholds associated with the 10 corresponding signal regions (EM1, EM2, ..., EM10) are shown in the second table of Fig. 1.2.

2.1 Object definition

Jets are recontructed following the anti-k_T algorithm [5] with a radius parameter $R = 0.4$, and only those jets with a transverse momentum p_T^j and pseudorapidity η^j satisfying

$$p_T^j > 20\,\text{GeV} \qquad \text{and} \qquad |\eta^j| < 2.8 \tag{1.4}$$

are retained. Among those jets, those with a transverse momentum greater than 30 GeV and with a pseudorapidity smaller than 2.5 (in absolute value) are potentially considered as b-tagged, according to a b-tagging working point that is in average 60% efficient [6].

Electron candidates are required to have a transverse momentum p_T^e and pseudorapidity η^e obeying to

$$p_T^e > 20\,\text{GeV} \qquad \text{and} \qquad |\eta^e| < 2.47\,, \tag{1.5}$$

whereas muon candidates must obey to

$$p_T^\mu > 10\,\text{GeV} \qquad \text{and} \qquad |\eta^\mu| < 2.7\,. \tag{1.6}$$

Any non-b-tagged jet with $p_T^j > 30$ GeV lying within a cone of radius $\Delta R < 0.2$ from an electron is discarded, whilst any electron lying within a cone of radius $\Delta R < 0.2$ centered on a b-tagged jet is removed. Any electron that would then lie within a cone of radius $0.2 < \Delta R < 0.4$ of a jet is finally removed in a second step. In addition, jets with a $p_T^j > 30$ GeV are discarded if they are lying in a cone of radius $\Delta R < 0.4$ centered on any muon.

The missing transverse momentum vector $\not{p}_T$ is defined as the opposite of the vector sum of the momenta of all reconstructed physics object candidates with a pseudorapidity smaller than 4.9, and the missing transverse energy E_T^{miss} is defined by its norm.

2.2 Event Selection

Event preselection imposes first the presence of a significant amount of missing energy,
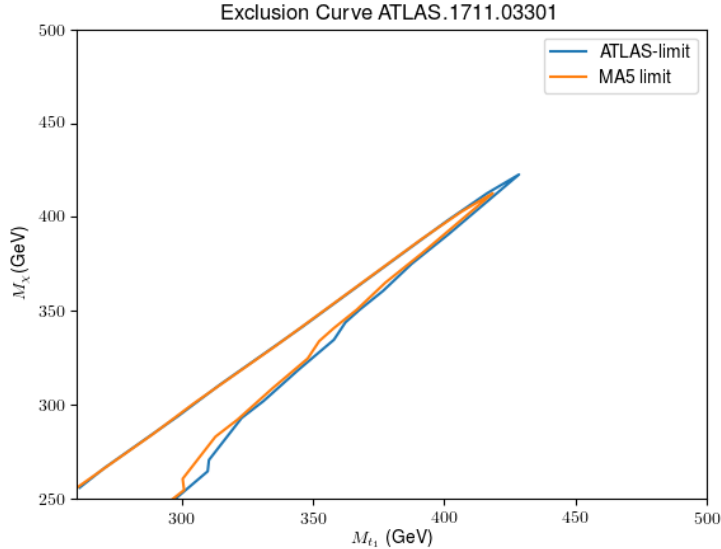
$$E_T^{\text{miss}} > 250\,\text{GeV}, \tag{1.7}$$

Fig. 1.3: Exclusion contour in the $(M_{\tilde{t}}, M_{\tilde{\chi}})$ plane of the considered stop-neutralino class of simplified model. We compare the MADANALYSIS 5 findings (orange) with the official ATLAS numbers (blue).

and next that the final state features a monojet-like topology, the leading jet being imposed to satisfy

$$p_T(j_1) > 250 \text{ GeV}. \tag{1.8}$$

Electron and muon vetos are then enforced, and any jet j has to be well separated from the missing momentum,

$$\Delta\phi(j, \not{p}_T) > 0.4 . \tag{1.9}$$

Selected events are then categorized into the inclusive and exclusive signal regions introduced in Fig. 1.2.

3 Validation

For our validation, we generate events for various simplified models inspired by the MSSM. We consider a class of models where the Standard Model is extended by a stop (of mass $M_{\tilde{t}}$) and a neutralino (of mass $M_{\tilde{\chi}}$), all other superymmetric states being taken decoupled. For each choice of mass parameters, our signal event samples are normalized to an integrated luminosity of 36.2 fb^{-1} and to a cross section evaluated at the NLO+NLL accuracy [7].

Signal events have been generated with MADGRAPH5_AMC@NLO [8] and PYTHIA 8 [9] for the hard scattering matrix elements and the simulation of the parton showering and hadronization, respectively. We have considered event samples describing final states featuring different jet multiplicities, that we have merged through the MLM scheme [10, 11]. The merging scale as been set, for each point, to $Q^{\text{match}} = M_{\tilde{t}}/4$ GeV for a MADGRAPH5 xqcut parameter set to 125 GeV. The A14 PYTHIA tune [12] has been used while showering and hadronizing events with PYTHIA 8, and the simulation of the ATLAS detector has been achieved with the DELPHES 3 program [13], assuming a b-tagging efficiency of 60% for a p_T-dependent mistagging rate equal to $0.1 + 0.000038 * p_T$.

In the absence of any official ATLAS cutflow for given benchmark scenarios, we have decided to validate our reimplementation by reproducing the ATLAS exclusion contour for a set of compressed benchmark points for which the stop decays as $\tilde{t}_1 \rightarrow c\chi_1^0$. Our results are presented in Fig. 1.3 in which we superimpose the exclusion contour obtained with MADANALYSIS 5 (orange) with the official

ATLAS one (blue). We observe an excellent degree of agreement, which makes us considering our reimplementation as validated.

4 Summary

We have implemented the ATLAS-EXOT-2016-27 analysis the MADANALYSIS 5 framework, an analysis searching for dark matter models in the monojet channel and in 36.2 fb^{-1} of ATLAS collision data at a center-of-mass energy of 13 TeV. In the absence of any detailed validation material, we have validated our reimplementation in reproducing the exclusion curve provided by ATLAS in the context of a class of simplified models where the Standard Model is extended by a neutralino and a stop that decays into the $\tilde{t}_1 \to c\chi_1^0$ channel. We have obtained an exceptionally good agreement, so that our reimplementation has been considered as validated.

References

[1] E. Conte, B. Fuks, and G. Serret, *MadAnalysis 5, A User-Friendly Framework for Collider Phenomenology*, *Comput. Phys. Commun.* **184** (2013) 222–256, [arXiv:1206.1599]. 5

[2] E. Conte, B. Dumont, B. Fuks, and C. Wymant, *Designing and recasting LHC analyses with MadAnalysis 5*, *Eur. Phys. J.* **C74** (2014), no. 10 3103, [arXiv:1405.3982]. 5

[3] B. Dumont, B. Fuks, S. Kraml, S. Bein, G. Chalons, E. Conte, S. Kulkarni, D. Sengupta, and C. Wymant, *Toward a public analysis database for LHC new physics searches using MADANALYSIS 5*, *Eur. Phys. J.* **C75** (2015), no. 2 56, [arXiv:1407.3278]. 5

[4] **ATLAS** Collaboration, M. Aaboud et al., *Search for dark matter and other new phenomena in events with an energetic jet and large missing transverse momentum using the ATLAS detector*, *JHEP* **01** (2018) 126, [arXiv:1711.03301]. 5

[5] M. Cacciari, G. P. Salam, and G. Soyez, *The Anti-k(t) jet clustering algorithm*, *JHEP* **04** (2008) 063, [arXiv:0802.1189]. 6

[6] **ATLAS** Collaboration, *Optimisation of the ATLAS b-tagging performance for the 2016 LHC Run*, ATL-PHYS-PUB-2016-012. 6

[7] C. Borschensky, M. Krämer, A. Kulesza, M. Mangano, S. Padhi, T. Plehn, and X. Portell, *Squark and gluino production cross sections in pp collisions at $\sqrt{s}$ = 13, 14, 33 and 100 TeV*, *Eur. Phys. J.* **C74** (2014), no. 12 3174, [arXiv:1407.5066]. 7

[8] J. Alwall, R. Frederix, S. Frixione, V. Hirschi, F. Maltoni, O. Mattelaer, H. S. Shao, T. Stelzer, P. Torrielli, and M. Zaro, *The automated computation of tree-level and next-to-leading order differential cross sections, and their matching to parton shower simulations*, *JHEP* **07** (2014) 079, [arXiv:1405.0301]. 7

[9] T. Sjöstrand, S. Ask, J. R. Christiansen, R. Corke, N. Desai, P. Ilten, S. Mrenna, S. Prestel, C. O. Rasmussen, and P. Z. Skands, *An Introduction to PYTHIA 8.2*, *Comput. Phys. Commun.* **191** (2015) 159–177, [arXiv:1410.3012]. 7

[10] M. L. Mangano, M. Moretti, F. Piccinini, and M. Treccani, *Matching matrix elements and shower evolution for top-quark production in hadronic collisions*, *JHEP* **01** (2007) 013, [hep-ph/0611129]. 7

[11] J. Alwall, S. de Visscher, and F. Maltoni, *QCD radiation in the production of heavy colored particles at the LHC*, *JHEP* **02** (2009) 017, [arXiv:0810.5350]. 7

[12] **ATLAS** Collaboration, *ATLAS Run 1 Pythia8 tunes*, ATL-PHYS-PUB-2014-021. 7

[13] **DELPHES 3** Collaboration, J. de Favereau, C. Delaere, P. Demin, A. Giammanco, V. Lemaître, A. Mertens, and M. Selvaggi, *DELPHES 3, A modular framework for fast simulation of a generic collider experiment*, *JHEP* **02** (2014) 057, [arXiv:1307.6346]. 7